

Learning to Super Resolve Intensity Images from Events

S. Mohammad Mostafavi I. *, Jonghyun Choi* and Kuk-Jin Yoon**

*Computer Vision Lab., GIST, Korea.

**Visual Intelligence Lab., KAIST, Korea.

mostafavi@gist.ac.kr; jhc@gist.ac.kr; kjyoon@kaist.ac.kr

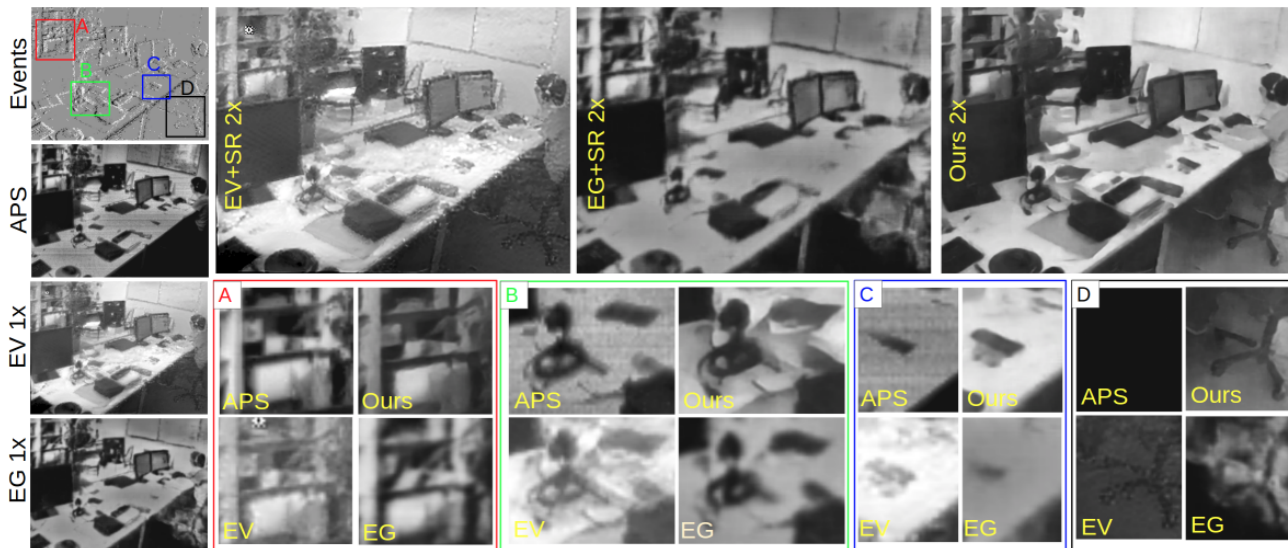


Figure 1. Reconstructing high-definition photo-realistic intensity images from pure events in end-to-end learning. Our events to super-resolved intensity image reconstruction recovers more details with less artifacts in comparison to recent methods of EG [23] and EV [17].

Abstract

An event camera detects per-pixel intensity difference and produces asynchronous event stream with low latency, high dynamic sensing range, and low power consumption. As a trade-off, the event camera has low spatial resolution. We propose an end-to-end network to reconstruct high resolution, high dynamic range (HDR) images from the event streams. The reconstructed images using the proposed method is in better quality than the combination of state-of-the-art intensity image reconstruction algorithms and the state-of-the-art super resolution schemes. We further evaluate our algorithm on multiple real-world sequences showing the ability to generate high quality images in the zero-shot cross dataset transfer setting.

1. Introduction

Event cameras have opened their path successfully to the computer vision and robotics society. Many new applications such as intensity frame reconstruction or recovering geometrical features such as optical flow or depth from the

event stream have emerged [1, 18, 11, 3, 21, 22]. The new device requires a new set of algorithms for existing vision tasks.

The event camera represents the changes of intensity for a specific pixel location (x, y) as a plus or minus sign (σ) asynchronously by checking the amount of intensity changes with a predefined threshold. This stream-like representation, depending on the scene and camera movement, can achieve μ s order of latency through accurate timestamps (t) . It is expressed per fired event in the form of (x, y, t, σ) . This device has gathered a lot of attention due to the high applicability in systems requiring high dynamic range outputs with low latency, and low power and low memory consumption constraints [15, 23, 17, 26, 5]. Moreover, event cameras can sense the events and intensity image on the same grid-line of pixels (usually the same size spatial resolution) and conveniently report both values [2].

Unfortunately, most commercially available event cameras have relatively low resolution events for their efficiency. While others have focused on intensity image reconstruction, depth estimation, optical flow estimation, video synthesis, localization and ego-motion estimation, and vi-

sual odometry, estimating super-resolved intensity images from pure events has been barely explored in the literature. Although the events can be transferred to intensity images and then converted to higher resolution images using existing super resolution methods [4, 20, 7, 14], we aim to directly learn to estimate pixel-wise super-resolved intensity from events in an end-to-end manner. We demonstrate that this direct implementation improves the overall quality of super resolved images with less artifacts and rich details.

To our best knowledge we are the first to model super-resolving event data to higher-resolution intensity images in an end-to-end learning framework. With the high frame rate of event stream we can generate super resolved frames both in terms of spatial and temporal resolution.

2. Related Work

We present a new task of directly estimating intensity images in a higher resolution directly from events, however to complete our overview, related work is divided into two subsections: event to intensity synthesis and image SR.

Event to Intensity Images. Early attempts in showing the applications of event cameras included considering relatively short periods of the event stream data and direct accumulation of the plus or minus events in two colors as a gradient interpreted output [2]. Synthesising intensity images instead of that representation goes back to the task of simultaneously estimating the camera movement and mosaicing them as a panoramic gradient image [11]. In their setting the scene is static and the camera only has rotational movements. By utilizing Poisson integration they eventually transfer the gradient image to an intensity image. In [3] a bio-inspired network structure of recurrently interconnected areas was proposed to predict different visual aspects of the scene such as the intensity image, optical flow, and angular velocity from small rotation movements. Bardow *et al.* proposed the joint task of estimating optical flow and intensity simultaneously in a variational energy minimization scheme in a challenging dynamic movement setting [1]. However, their method suffers from error propagation and also creates shadow-like artifacts on the intensity images.

A variational framework based on a denoising scheme that filters the incoming events iteratively was introduced [18]. They utilized manifold regularization on the relative timestamp of events to reconstruct the image being able to create more grayscale variations in untextured areas. In [21], an asynchronous high-pass filter was proposed to reconstruct computationally efficient videos. This framework was initially designed for complementing intensity frames with the event information but was also capable of reconstructing images from pure events.

The more recent trend in intensity image synthesis is using deep convolutional networks in which they are capable of creating photo-realistic outputs directly from the event

stream [23], [17]. They both follow a *U-net* structure [19] as the base network with modifications such as using conditional generative adversarial neural networks [23], or using a deep recurrent structure (up to 40 steps) together with stacked ConvLSTM gates [17]. They further invested the possibility of reaching very high frame-rates and using the output intensity images for downstream applications.

Image Super-Resolution. Intensity image SR can be divided into single image SR (SISR) [4, 14] or multiple image SR (MISR) or also known as video SR [20, 7]. MISR uses a sequence of images over time therefore it generally is more successful in recovering missing details and higher frequency information. Since we have a stream of events over time video SR can be considered the most similar field of interest, although we aim to reconstruct one single image each time. Many of these learning based SR methods outperform previous methods by using deeper and wider networks while utilizing the power of residuals to prevent vanishing gradients [14, 7]. Many MISR techniques also use optical flow representations among the input images as a supplementary source of input to reach higher quality SR outputs [20, 7]. Inspired by these methods we design our SR sub-network as explained in Sec. 4.

3. Approach

We first assume that an event is a highly abstract representation of the underlying scene. The level of abstraction is higher than the same sized intensity image thus it requires to transfer accumulated information to a media with higher capacity such as a super-resolved intensity image for better visibility. It implies that a direct transformation from event to high resolution intensity images is preferred to generate high quality images than a pipelined approach of generating a low resolution intensity images from images followed by a super-resolving method, which leads to a sub-optimal solution.

We propose an end-to-end framework to generate the super-resolution images from event streams. Specifically, each part of the event stream stacked based on the number of events to contributes as a hidden state which transforms to some part of the whole scene, while the temporal relation between each of contributing stacks can be determined based on its optical flow. Beginning with event stacking strategy, we describe our network architecture.

3.1. Event Stacking Strategy

The raw stream-like representation of events cannot be directly used as an input for the network as it is sparse in spatial domain and needs preparation. Following the stacking notations in [23], we mainly use the stacking based on the number of events (SBN) as it follows the intrinsic logic of the event camera. This stacking allows us to create a very

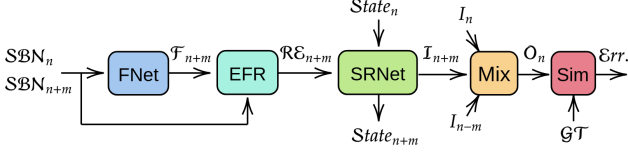


Figure 2. Network structure of our event to super-resolved intensity image framework. The input stacks SBN_{n+m} and the central stack SBN_n are given to the FNet to create the optical flow (F_{n+m}). The flow and stacks are concatenated and given to the EFR to rectify the event features. Its output RE_{n+m} is given to SRNet together with the previous state ($State_n$) to create intensity-like outputs I_{n+m} and the next state ($State_{n+m}$). All intensity-like outputs are concatenated and given to the mixer (Mix) network which creates the final output (O_n). Finally, the output is compared to the training GT using the similarity loss (Sim) which includes perceptual similarity (PS) network and the $\ell 1$ norm to create the final error (Err).

high frame rate by changing the amount of events fed to each stack and also the amount of shared events overlapping between each stack over time. Note that any event stacking method can be used in our framework although very recent works show it is beneficial to invest in the stacking methods [5, 22] which we will in future.

In our dataset we synchronized the starting point of the event stack at the same timestamp of the APS image and used past and future events from that point to make the rest of the wanted stacks as shown in Fig. 2. At inference, we can start from an arbitrary point in the event stream since the APS frames are not required.

Theoretically, since the network learns the relations from a lower scale abstract representation to a higher one, the relative size of the training pairs is important, not the absolute size. We empirically use 2, 500 events per stack in which each stack is a combination of 3 channels. This follows the average number of events in stacks that were able to show visually plausible outputs while keeping fine details. We change this number accordingly for our experiments with larger resolution event inputs. Since the network is trained on many diverse scene movements which creates different amount of local events, the network is robust to the chosen number of events per stack at inference.

3.2. Network Architecture

We have three principles in our architecture design. First, (1) defining the objective and designing based on the characteristics of the input and targeted output. The *event stream* holds all the information from the parts of the scene that have had enough gradient to trigger positive or negative event thresholds. That is the reason that some parts of the scene might not be visible near the timestamp we intend to reconstruct the intensity image. Furthermore, the event stream itself is actually a continuous sequential representation of the captured scene. Therefore a network that can

handle a sequence-like stream recurrently will be more effective. In such network, each stack can contribute partially to the overall output. Accordingly, we propose a recurrent-based network architecture as expressed in Fig. 2, where we further visualize its inputs, intermediate optical flow, and intensity-like results plus the final output as Fig. 3. Although this diagram specifically visualizes our method when having three stacks ($3S$) as the input sequence, it can be generalized to any number. The three stacks are: the stack containing the APS timestamp SBN_n , the stack after it SBN_{n+m} and the stack before it SBN_{n-m} .

Suppose a stream of events starting from the timestamp of the n th APS frame (GT intensity image). Each stack has M (e.g. 2, 500) events and its end location m will vary on the timeline of events based on the amount of time it is required to fire M events. SBN_n is the the stack having $M/2$ events before and $M/2$ events after this location. This is the second stack from the sequence of three which is fed given to the network after SBN_{n-m} and we call it the central stack since the predicted intensity output will have the most resemblance with this stack and also each previous or next stack is compared to this stack when predicting the optical flow by *FNet*. The next two stacks are M events away from the end of the previous stack ($M/2$) if no overlap ($L = 0$) is considered as the stacks of Fig. 3. We can also have overlapping stacks for creating higher frame-rates, in that case the end of the next stack will be M events after the center minus the amount of overlap ($M/2-L$). The previous or next stack is given individually with the central stack to the optical flow estimation network (*FNet*) to predict the optical flow (F_{n-m} or F_{n+m}) between these two stacks.

The stacks of events infused with optical flow (by *FNet*) are concatenated and then rectified by an event feature rectifier (*EFR*) progressively. *EFR* perceptually acts as an event feature rectifying module and extracts features from the three concatenated inputs. The rectified event stack (RE_{n+m}) is then given to the SR network (*SRNet*). This network takes the previous state ($State_n$) together with the rectified events stack and creates the next state ($State_{n+m}$) of the sequential model and a super-resolved intensity like output (I_{n+m}). This output together with the past and central intensity-like prediction (I_{n-m}, I_n) is given to a mixer network that concatenates all the inputs and passes them through the final convolutional stage. Note that for the first hidden stage, the first stack is given directly to the *EFR* sub-network to create an initial $State_n$.

In the best case, each stack contributes to detailed structures mainly from locations which contain events to the final output. The overall parts are then mixed in a final stage to create the output intensity image O_n . When training, this output is given to the network known as the perceptual similarity network (Sim) to get one part of the optimization criterion's error (Err).

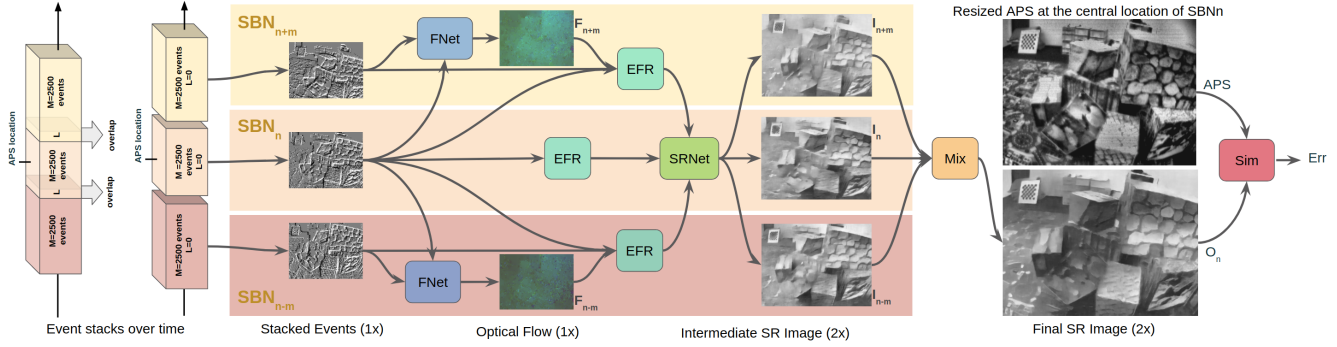


Figure 3. Overview of the proposed method. This example is based on third stack (SBN_{n+m}), therefore the previous inputs, optical flow, and intensity-like outputs are faded. The APS frame is resized to the size of output (O_n) for comparison

Now, we implement the next two principles in the detailed network design described in the rest of this section: (2) having a suitable hypothesis space in terms of the learned parameters which will be explained in the super-resolution network (SRNet Sec. 3.2.3) and (3) optimizing a task-specific criterion (Sec. 3.2.5).

3.2.1 Flow Network

An unwanted downside of stacking the event stream is losing the temporal relation among stacks. This can be recovered to some extent by using a sequence of the stacks with their inter-related optical flow. The event stack representation by itself can be a useful input to well-known learning-based optical flow estimation algorithms. We use [9] as our flow estimation network and call it FNet. Theoretically the chosen optical flow algorithm should not have much influence on the overall training procedure because this given flow representation acts as an input to the rest of the network. For that reason, this network is not necessarily required to be included as a trainable parameter and is excluded for reducing the number of parameters and easier convergence.

3.2.2 Event Feature Rectification Network

Another downside of stacking events is overwriting previous event information on fast triggering locations. This gives a blurry stack of events which later results in lower quality reconstructions. To prevent that, we concatenate two stack of events with the optical flow and give it to two convolutional layers called the event feature rectification sub-network. Note that instead of concatenating a large combination of event stacks at once, we progressively fuse the stacks over the event stream to ensure maximum production of intensity features from the presence of each event. Furthermore, if two stacks have non-related events in a location visible to one stack only, it will still be used for the intensity reconstruction since we have concatenated all three inputs.

3.2.3 Super Resolution Network

It has been generally shown that stacked events are capable to be synthesized to intensity images through deep neural fields [23, 17] such as *U-net* [19]. We further extend the idea by using *ResNet* [8] with 15 blocks in depth with more filters and larger kernel size. Its main task is to create an initial SR intensity image state through the combination of transposed convolutional operations. We use large field of views as our patches inspired from the SISR network from [6] to create out rectified event feature to SR intensity output generator (*RNet-C*). Following the well-designed networks in MISR [14, 20, 6, 4] we utilize the power of residual learning for super-resolving features through the network.

We use the combination of three residual networks ($RNet\{A, B, D\}$) in which each contains 5 ResNet blocks containing two convolutional layers. These networks are less deep in comparison to *RNet-C* because they already hold feature-like representations from previous states and not directly from the event stacks. The output of *RNet-A* which also acts as an upsampling encoder is subtracted with the output of *RNet-C* to create an internal error state (e_n) which shows how much the current rectified event stack RE_{n+m} contributes in comparison to the previous state $State_n$ as

$$e_n = RNet-C(RE_{n+m}) - RNet-A(State_n). \quad (1)$$

This error is given as an input to *RNet-B* which acts as a general encoder. The output of *RNet-B* and *RNet-C* are eventually summed so the current input will have the most emphasise rather than the previous state as

$$State_{n+m} = RNet-B(e_n) + RNet-C(RE_{n+m}). \quad (2)$$

This summation creates our next state ($State_{n+m}$) and is given to a final decoder (*RNet-D*) to make the intermediate intensity-like output (I_{n+m}).

$$I_{n+m} = RNet-D(State_{n+m}). \quad (3)$$

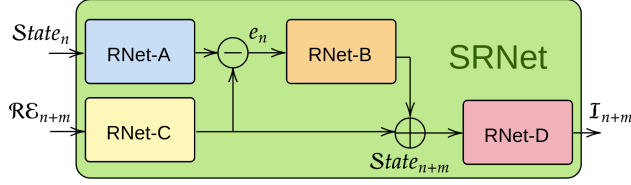


Figure 4. Detailed architecture of the proposed super resolving network (SRNet) (Green-block in Fig. 2). Four main residual networks are designed to perform as a large encoder-decoder scheme. *RNet-A* is used to update the hidden state while *RNet-B* and *RNet-D* act as an encoder and decoder respectively to decipher the hidden state as a super resolved intensity output (I_{n+m}).

In an ideal setting, *RNet-C* adds new information to the previous state by adding missing details of the scene. If the new stack misses some information due to lack of camera or scene movement where no event triggers, the previous state holds that information through *RNet-A* as its hidden state. Further design parameters are included in the supplementary material.

3.2.4 Mixer Network

This sub-network is designed to collect the outputs (I_i) of the SRNet at different stack locations ($i=\{n-m, n, n+m\}$) and give one final output intensity image (O_n) based on the center location (n). This network consists of a concatenator which concatenates all the outputs of the SRNet and then feeds them to a final convolutional layer to reconstruct the photorealistic intensity output.

3.2.5 Similarity Loss

The last principal to reach higher quality outputs is optimizing a task-specific criterion. Given a synthesized image (x) and its GT (y), the usual trend is training a network using an unstructured loss such as the ℓ_1 norm (which encourages less blur in comparison to ℓ_2). Which mainly results in smoothed edges with less high frequency texture in output images as

$$\mathcal{L}_{\ell_1}(x, y) = \|SR(x) - y\|_1. \quad (4)$$

Therefore, we further leverage a criterion capable of compensating the lack of structure. The second loss is formed as the perceptual similarity (PS) metric [25] over the high level features of the input images instead of directly comparing them. Given a pair of images (x, y) to a pretrained network (e.g., AlexNet [12]), the near end features (\hat{y}_{hw}^l) of the L -th layer are extracted while its activations are normalized through the channel dimension (H_l, W_l). Then each channel is scaled by vector w_l , and the ℓ_2 distance is calculated. Finally the mean value is calculated across the image dimension (h, w) through all layers (l) to get the perceptual

similarity loss as

$$\mathcal{L}_{PS}(x, y) = \sum_l \frac{1}{H_l W_l} \sum_{h, w} \|w_l \odot (\hat{x}_{hw}^l - \hat{y}_{hw}^l)\|_2^2. \quad (5)$$

We use the combination of ℓ_1 norm and PS as

$$\mathcal{L}_{sim} = \operatorname{argmin}_{x, y} \lambda \mathcal{L}_{\ell_1}(x, y) + \mathcal{L}_{PS}(x, y). \quad (6)$$

3.3. Dataset

To make pairs of event and higher resolution intensity images, we can either use an event camera paired with an intensity camera and warp both to the same center of camera, or use an event camera that reports the intensity and event together in one device by considering the active pixel sensor (APS) frame as ground truth (GT). The event camera however needs movements of the scene or the camera to sense the scene. Under normal conditions, movements create motion blur on the intensity image. Furthermore real-world noise will have a different effect on intensity and events. Moreover the dynamic range of an event camera and an intensity camera are much different which one device might sense parts of the scene the other device misses. The combination of these reasons makes real-world sensing devices prone to major errors when used as the training source.

Furthermore, when working with the same resolution intensity and event device for creating low resolution (LR) event and high resolution (HR) intensity pairs, one might think of resizing the event data to a smaller value. This might work on the training set but when generalizing to the test set that does not have such resized inputs such as the original events of the event camera, the outputs will have much lower quality. The reason behind it is that subsampling algorithms leave unwanted traces on the event stack. This effect might seem negligible, but in a learning based solution, it leads to erroneous parameters. In our experiments subsampling the events resulted in a drop of almost $2dB$ in terms of PSNR. This is a crucial step to reach higher quality outputs for cross evaluating on other datasets which we set as a goal.

To create training dataset, we use the event camera simulator (ESIM) [16] To be immune to the mentioned down-sampling flaw, we utilize a pair of cameras with different resolutions. The LR (event) camera has 64×64 pixels resolution and the HR intensity camera has 128×128 or 256×256 pixels based on the upscale factor ($2 \times$ or $4 \times$), both sharing the same camera center. To have exactly the same field of view in both cameras without further warping requirements, the focal length is multiplied to the desired upscale factor when moving from the LR event camera to the HR GT intensity camera.

We created our dataset using 1,000 different images placed on a planar surface while moving the cameras in 6-DoF on top using random trajectories and created almost

120K sequences of stacks. Different cameras can have different threshold values, therefore we randomly set the positive and negative threshold independently for each sequence to prevent the network from adapting to this parameter therefore being versatile to the input source. Although we train using simulated events, we experimentally show that we can fully transfer to real-world scenes without any fine tuning in a complete blind dataset transfer setting.

4. Experiments

We use PSNR in dB (logarithmic scale), the structural similarity [24] (SSIM) as a fraction between zero (less similar) to one (fully similar), and the mean squared error (MSE) for the quantitative metric for comparison in all experimental validations. We also use the perceptual similarity as a metric to evaluate the similarity of the high level features in two images (lower value means more similar). For each experiment, we train our network for 50 epochs (about 6 million iterations) on a cluster of 8 NVIDIA Titan-X GPUs.

4.1. Comparison with State of the Arts

We continue our experiments by comparing our method to recent methods. In addition to the created simulated sequences, we further test on a combination of four challenging and diverse real-world online available datasets [1, 15, 21, 26] expressed in this section and the supplement.

To be able to show our performance, we first compare our intensity reconstruction to the top recent algorithms in this field. Then, we compare the task of SR as a downstream application to intensity image reconstruction. In our experiments, we abbreviate the High pass Filter method [21] as HF, Manifold Regularization [18] as MR, Event to Video generation [17] as EV and Event to intensity by utilizing GANs as EG [23]. We use seven challenging real-world sequences from the event camera dataset [15].

There is a mismatch between the APS frame and the GT making the APS frame an unreliable source (refer to Sec. 3.3). But that is the best available data near the GT in many datasets. The mismatch has the more effect on direct distance-based metrics (PSNR, SSIM and MSE), therefore we only utilize the PS value for comparison in such cases. We use the sequences of [15] as a reference for intensity image synthesis. We follow the sequence split of [17] and use his reported numbers for HF, MR and EV. For EG, we used the author’s reconstructed images and evaluate them. We downsample our results when comparing to the non super-resolved methods. Based on Table 1, our proposed method has the lowest number in terms of PS which means we reconstruct intensity image perceptually better than the previous methods over each sequence and in average. It is noteworthy to mention that we only trained with synthetic data and reached the highest performance on real-world events through zero-shot transfer training on

Table 1. Event to intensity synthesis comparison using Perceptual Similarity (PS). Our method outperforms the previous methods in all sequences. The runner up method is underlined.

Seq. \ PS (↓)	HF [21]	MR[18]	EV[17]	EG[23]	Ours
dynamic_6dof	0.54	0.50	<u>0.46</u>	0.56	0.42
boxes_6dof	0.50	0.53	<u>0.38</u>	0.39	0.32
poster_6dof	0.45	0.52	<u>0.35</u>	<u>0.35</u>	0.29
shapes_6dof	0.61	0.64	<u>0.47</u>	0.56	0.38
office_zigzag	0.54	0.50	<u>0.41</u>	0.44	0.29
slider_depth	0.50	0.55	<u>0.44</u>	0.48	0.34
calibration	0.48	0.47	0.36	<u>0.34</u>	0.24
Average	0.52	0.53	<u>0.41</u>	0.45	0.33

real-world events. The two runner up methods (EV and EG) also create semi-photo-realistic outputs and are both deep-learning based methods. Qualitative comparison among the top three methods are available in Fig. 1 and 6. When qualitatively comparing these images, EG does not always follow the events and sometimes hallucinates non-related jittery artifacts. Although EV follows the events relatively better, it creates a shadow-like artifact that follows the events and darkens some areas of the scene. Furthermore, in EV the events themselves are quite visible sometimes as white or black dots. Our outputs are free from such artifacts.

EV is the runner up method that performs better than EG in most of the sequences and overall in average. Furthermore in the implementation of EV temporal consistency is utilized which enables using MISR methods easier. Therefore we only use the reconstructed images from EV to perform the SR experiments using their online available algorithm. We try the task of using reconstructed intensity images as an input to two recent SISR [4] and MISR [7] algorithms. We use 30 sequences from our dataset (explained in section 3.1) which were excluded from the training for testing purposes. In Table 2, although using an intensity reconstruction algorithm in combination with other downstream applications might give acceptable results to some extent, however much higher quality results can be obtained when directly super-resolving from events. To get a more qualitative comparison on this combined scheme, we compare intensity reconstruction of EV and the combination of EV+MISR outputs on real-world and simulated sequences in the Fig. 6. Our method reconstructs higher quality fine details from events. More results are available in the supplementary material.

We further perform experiments on the scenes from [1] in Fig. 5 and compare to EG and EV visually. In these sequences, we can visually approve the idea that mapping to a higher resolution grid can be beneficial for intensity image reconstruction. Through our strategy we can slightly reveal structure that is not visible when aiming for the same size resolution such as fingertips or texture details.

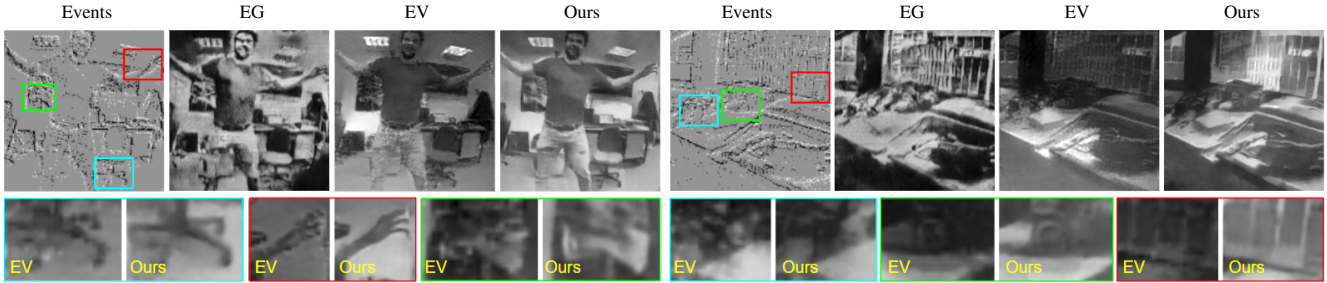


Figure 5. Qualitative comparison of our downscaled outputs to EV and EG on sequences from [1] (without APS). Our method is able to reconstruct structural details from inputs as small as 128×128 pixels. More sequences are provided in the supplementary material.

Table 2. Quantitative comparison of super-resolved intensity images from events directly (Ours) to events to intensity image synthesis (EV) combined with different SR (SISR [4], MISR[7]) methods

Method	PSNR (\uparrow)	SSIM (\uparrow)	MSE (\downarrow)	PS (\downarrow)
EV + MISR 2 \times	11.309	0.385	0.347	0.392
EV + SISR 2 \times	11.292	0.384	0.348	0.394
Ours 2 \times	16.420	0.600	0.108	0.172
EV + MISR 4 \times	11.293	0.384	0.087	0.396
EV + SISR 4 \times	11.168	0.396	0.089	0.543
Ours 4 \times	16.068	0.560	0.028	0.253

Table 3. Ablating different components of the loss function.

Similarity	PSNR (\uparrow)	SSIM (\uparrow)	MSE (\downarrow)	PS (\downarrow)
ℓ_1	15.33	0.517	0.034	0.485
PS	10.06	0.388	0.454	0.232
$\ell_1 + PS$	<u>15.03</u>	0.528	0.032	<u>0.258</u>

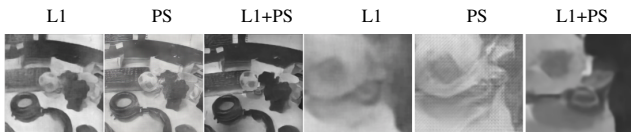


Figure 8. Effect of loss function on reconstruction quality. ℓ_1 norm smooths edges, perceptual similarity (PS) adds structural details but also creates artifacts. The combination of $\ell_1 + PS$ shows less artifacts while adding structural details.

4.2. Ablation Studies

We ablate the effect of different loss factors on image reconstruction quantitatively in Table 3 and qualitatively in Fig. 8. All of our network ablation studies were performed only using simulated data with reliable high quality output intensity images. The ℓ_1 norm has higher quality metrics but leads to less visually sharp images. The PS loss creates images that look visually acceptable but with the downside of lower PSNR plus dot-like artifacts on regions with less events and on the edges. The combined loss gets the best from both and creates visually plausible images with a slight decrease in PSNR but overall improvement on other metrics.

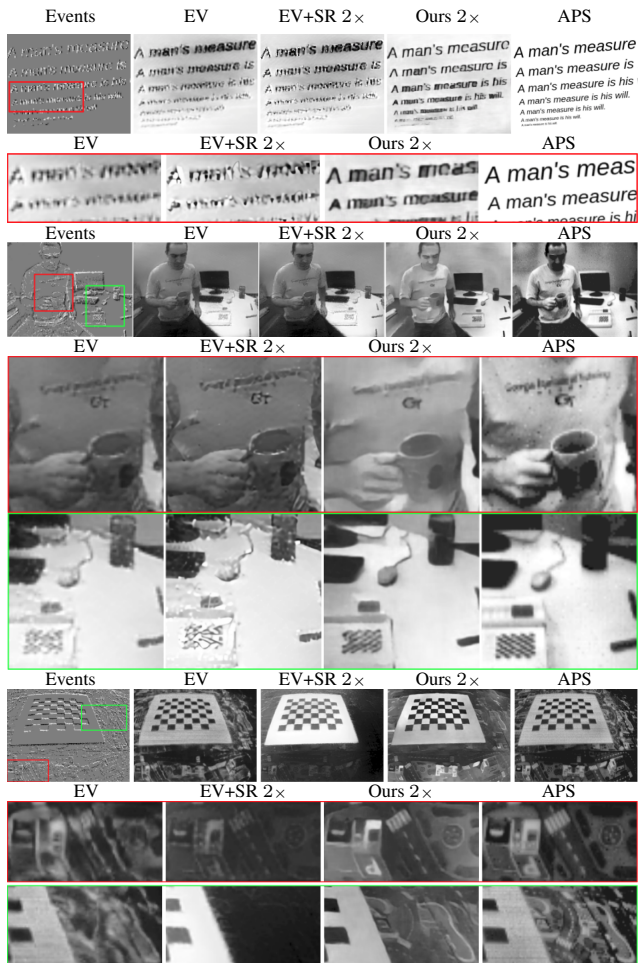


Figure 6. Comparison among synthesizing SR intensity images directly (ours) and super-resolving as a downstream application to intensity image estimation (EV+MISR). Highlighted boxes are zoomed for better comparison.

We evaluate the effect of the upscale factor ($2\times$, $4\times$) and size of the sequence of stacks ($3S$, $7S$) on the output intensity images in Table 4. Comparing $3S$ and $7S$ is actually observing the effect of having a longer recursion on the sequences with more reliability on the hidden state. Theoretically this can be helpful for the case of synthesizing images

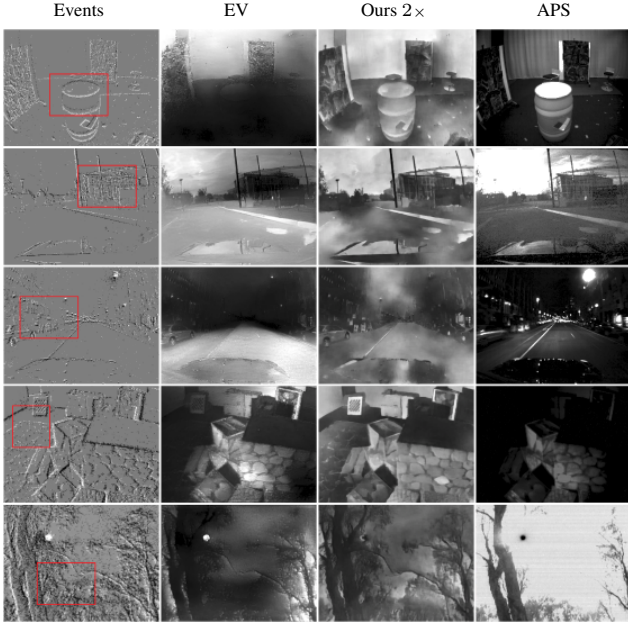


Figure 7. Expressing the robustness of our intensity image reconstruction in challenging scenes. When testing on diverse indoor and outdoor scenes with different lighting conditions and extreme HDR scenarios [21, 26, 15], our method synthesizes more details while producing less artifacts in comparison to EV and the APS. Please zoom in and compare the suggested regions.

Table 4. Effect of number of stacks and scale factor.

Scale	# Stacks	PSNR (\uparrow)	SSIM (\uparrow)	MSE (\downarrow)	PS (\downarrow)
2 \times	3S	15.46	0.554	0.323	0.191
	7S	16.42	0.600	0.108	0.172
4 \times	3S	15.03	0.528	0.032	0.258
	7S	16.06	0.560	0.028	0.253

directly from event stream since the camera can only view regions where enough movement from the camera or the objects in the scene are available. If an event belonging to some region only fires at a short period of time it can be easily neglected as we move away from that event through time. However unrolling on a larger recursion helps to keep that small amount of events effective for the final intensity image reconstruction. Increasing the scale factor does not necessarily improve the quality, possibly due to the inability of the algorithm to handle large spatial locations where no events exist. Although the MSE has decreased, but this goes back to the larger number we get in the denominator related to the size of the image and not much related to the output quality. The next important factor is that using more stacks in a sequence actually improves the output quality specifically in terms of PSNR and PS. A larger sequence of stacks keeps short time firing events inside the hidden state, therefore increases the output quality.

Our main limitation is related to the number of stacks in a sequence which at the moment was hard to pass due

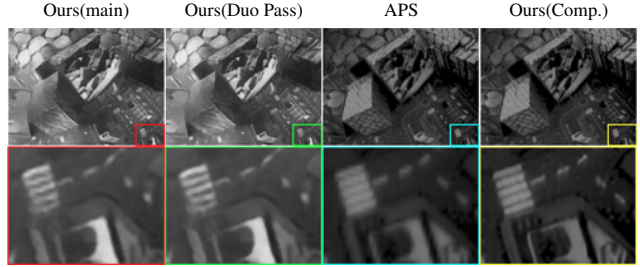


Figure 9. Extensions of our method. Complementary (event+APS) SR or dual passing to complementary network after main synthesis (event only) is compared to the main method and APS frame for reference.

to GPU memory shortage. Failure cases are mainly related to missing background details over long trajectories when the foreground objects have rapid movements. In such sequences, our method can only recover parts of the scene that are in a limited time distance to our central stack. Sample outputs are showcased in the supplementary material.

5. Extensions

We further extend the idea of using the APS frame and events as complementary sources [21] as synthesizing a super-resolved intensity images using our framework. In a separate setting, we trained the initial state of network with the LR APS frame (as the central stack) and gave the events as its consecutive following stacks. In this manner the network learns to add higher resolution details to the LR intensity input. The problem with this framework is that the network is sensitive to the input image and if the input LR image is blurred or noisy it will be propagated to the final reconstruction. To solve that shortcoming, we implemented another follow-up approach as double passing. We give the output of our original approach and create intensity images from pure events. Then as the second pass, we use the newly mentioned complementary application and pass the synthesized intensity image to it. In this way, we are able to further recover HR details that the first pass misses. A sample output of each extension is shown in Fig. 9. Please refer to the supplementary material for more details.

6. Conclusion

We present the new task of directly reconstructing higher definition intensity images from pure events and propose a robust learning based solution to it. Our demonstration shows superior outputs in comparison to reconstructing the same size resolution outputs or creating low resolution images and super-resolving them as downstream applications. Targeting for a higher size canvas is beneficial for recovering small details when utilizing deep neural fields for event to intensity image estimation.

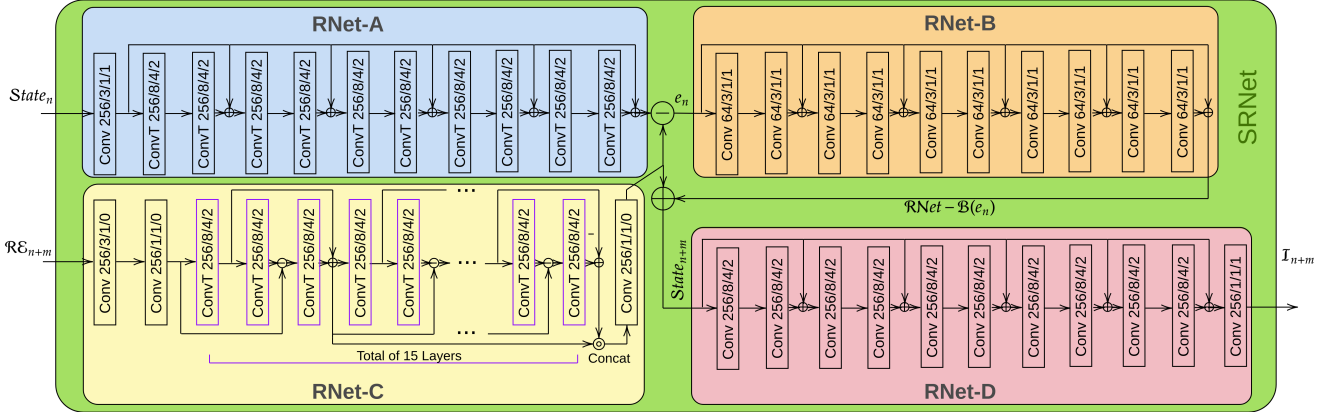


Figure 10. SRNet in detail components. Colors following Fig. 4

A. Design Parameters for SRNet (Section 3.2.3)

In Fig. 10, the text in each box indicates layer type, number of filters, kernel size, stride and padding respectively (e.g. Conv 64/3/1/1). The projection-wise setting of the recurrent residual modules follows the well-known iterative procedure for super-resolving multiple LR features called back-projection [10]. Although the original back-projection algorithm was proposed for known relative displacements, the idea of mapping a HR representation back to the LR feature is improved and integrated in recent SR techniques [20, 6, 7]. We adopt the idea to design our *SRNet*; more specifically *RNet-B* performs back-projection from RE_{m+n} to $State_n$ for producing the residual $RNetB(e_n)$.

B. Additional Comparative Results to the State of The Arts

We present more results on real-world and simulated sequences in Fig. 11, 12 and 13.

C. Additional Ablation Studies

C.1. Optical Flow

Stacking events by definition causes loss of temporal relations among events. Therefore we utilize FNet in our design to recover that loss by infusing optical flow by following that optical flow has been used in recent MISR techniques for inter-relating images over a sequences [20, 7]. In order to show the usefulness of optical flow on our intensity reconstruction, we ablate its effect by removing it as shown in Table 5. The base network is design for $4\times$ scale and $3S$ stacks with ℓ_1 norm only as the optimization criterion.

C.2. Effect of Number of Events Per Stack

The number of events in each stack affects the output reconstruction as shown in Fig. 14. When the number of event are around 2, 500 events for image sizes of 240×180

Table 5. Ablating the existence of FNet. Adding FNet to ℓ_1 improves all metrics. In the main paper all experiments included FNet and all ablations where performed using $4\times$ scale and 3 stacks ($3S$).

Similarity	PSNR (\uparrow)	SSIM (\uparrow)	MSE (\downarrow)	PS (\downarrow)
without FNet	14.97	0.505	0.036	0.499
with FNet	15.33	0.517	0.034	0.485

the output is generally in a reasonable quality and is even robust to accepting more events or missing less. However, adding much more events creates shadow-like outputs or blurred regions. Having much less events results in faded regions due to lack of information. Depending on the scene complexity, more or less events will be required.

To prevent overriding events in cases such as the shapes on bottom last row we stop adding events to the stack if a specific pixel gets overwritten more than 50 times and continue with the next stack in the sequence. This is the general automated process while hand-tuning this number might get better results for specific cases.

These examples further show that the APS frame is not a good reference for comparing the reconstruction of events in terms of low dynamic range, motion blur and locations where events exist and there is no intensity details corresponding to it (under the table in the 3rd row) or locations where image details exist but no events have fired (tape and paper detailed areas around the shapes in the last row).

D. Details on Extension Applications

D.1. Complimentary

The complementary extension uses the available APS frame and the events together to make a higher resolution intensity image by fusing the best from both sources. The training process for the main manuscript’s method is shown for seven stacks in a sequence ($S7$) in the green section of

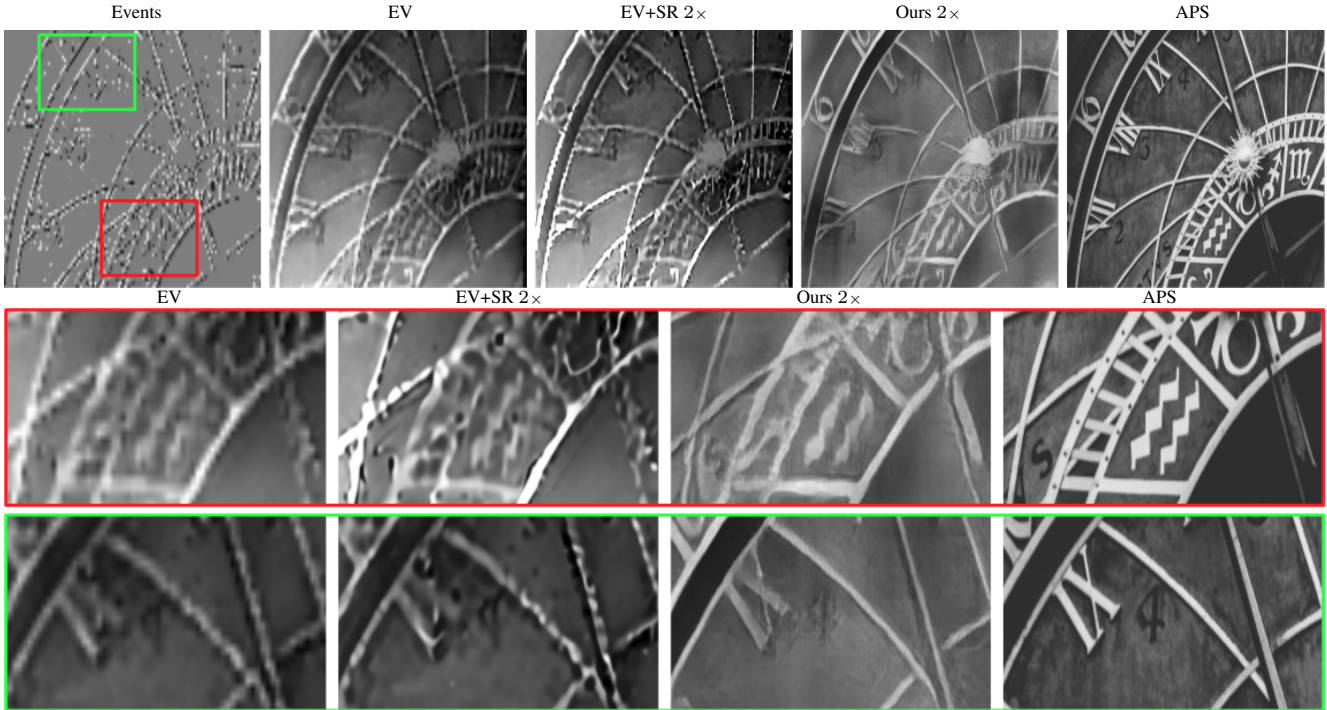


Figure 11. Additional comparison between direct event to SR intensity (ours) and event to image to SR intensity in a hierarchical manner (EV+MISR) on a simulated sequence. (In addition to the Fig. 6)

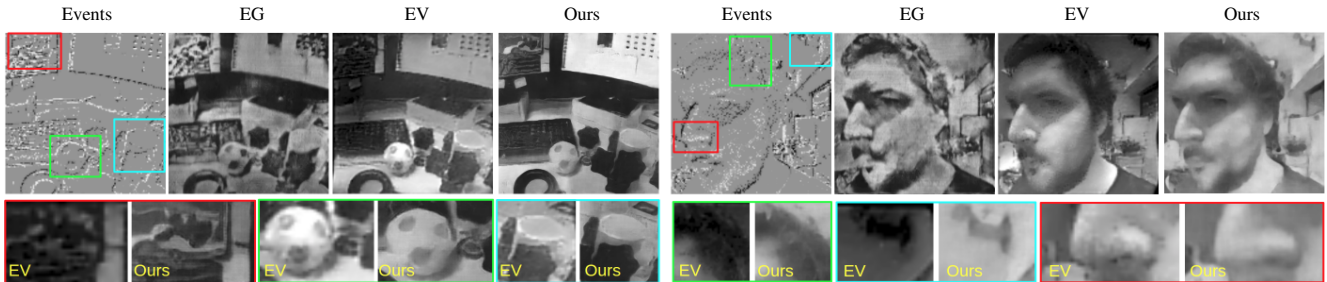


Figure 12. Additional comparison between EV, EG and our results on sequences from [1] (In addition to the Fig. 5).

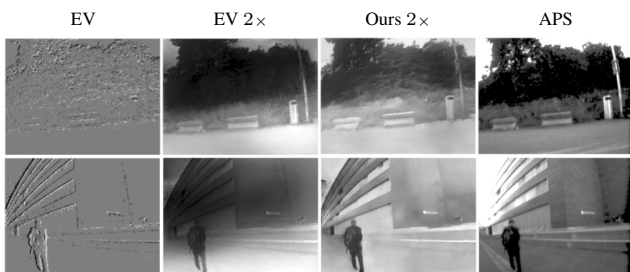


Figure 13. Intensity reconstruction in the presence of background noise from far away objects. (In addition to the Fig. 7)

Fig. 15.

The central stack is highlighted in the middle (SBN_3). The complimentary training also follows the same process but instead of events as a central stack it has the low resolution version of the GT. This time each previous or next

stack will be fused with the LR GT (APS) and fed to the network. At inference each event frame will add further HR details to the LR APS frame creating a super-resolved high quality output. Further results are shown in Fig. 16. If we use the APS frames we can only reach up to the frame rate of the APS. Furthermore, if the LR APS is noisy and blurry, this effect will be propagated to the output image.

D.2. Double Passing (Duo Pass)

The complimentary method is not pure event based and requires LR APS frames. However our main method is able to produce high quality intensity images from pure events without being effected by direct capturing noise or motion blur and is able to create crisp sharp edges. Furthermore, is we leverage the higher frame-rate creation algorithm we are not limited to any frame-rate and can create arbitrary

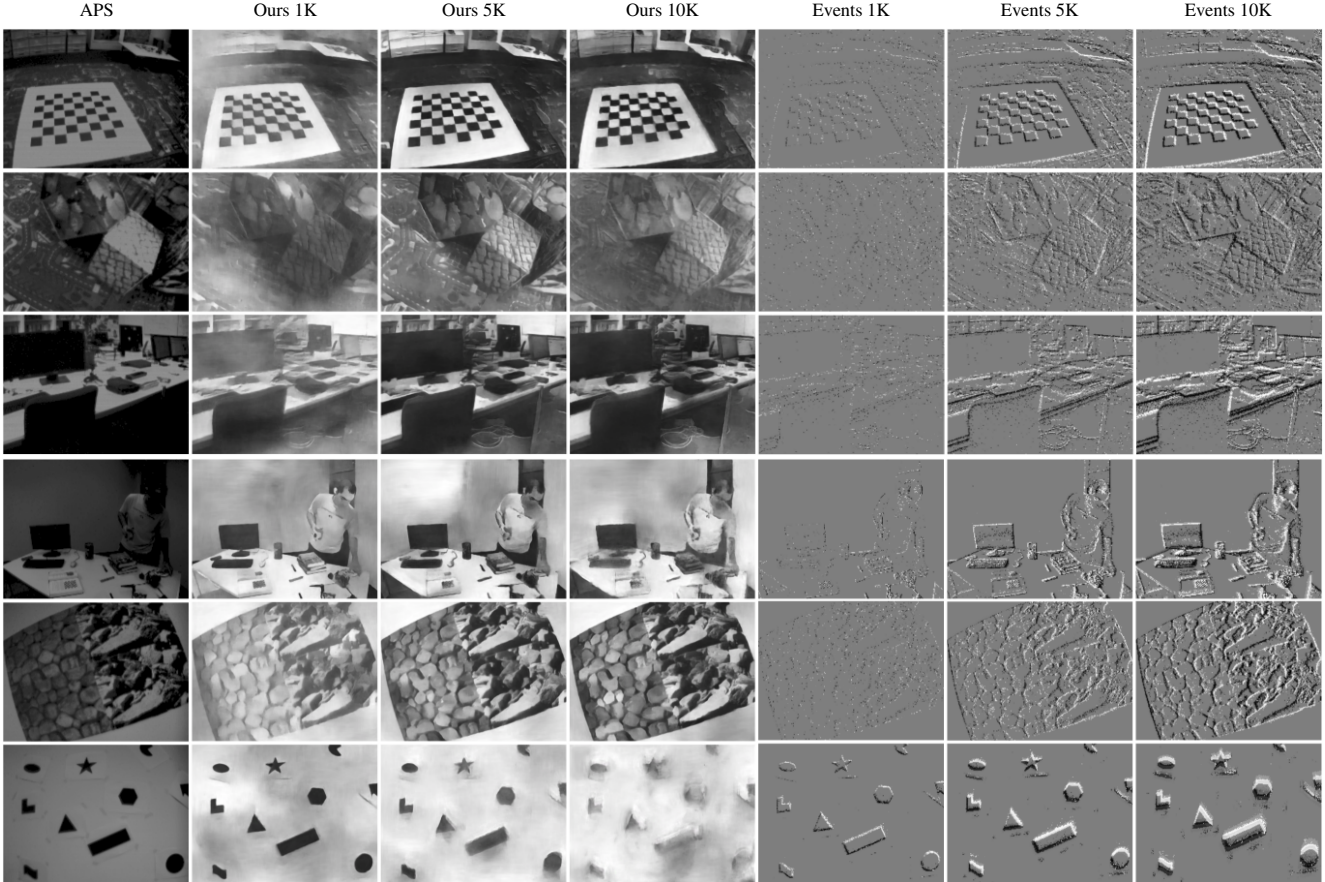


Figure 14. Effect of the number of events on reconstruction quality. APS frame shown is for reference.

frame-rates. Therefore, if we utilize these outputs as the LR images in the complimentary extension, we can solve the noise and blur propagation and remove the frame-rate limitation. As in Fig. 15, we just place the central stack (or frame) of the complimentary method with the synthesised intensity image of our main method. We call this method double passing (Duo-Pass) as expressed in Fig. 16.

E. Limitations and Failure Modes

Since the largest number of stacks in a sequence we implemented was $S7$, we are not able to currently recover all of the farther events in a sequence. Therefore our algorithm misses some background detail when fast foreground moving objects fire events. We are limited to the number of GPUs at our current implementation, but have plans to implement longer sequences. Fig 17 expresses a sample condition shown in a sequential manner over time.

Furthermore if the events in a stream are noisy or dead pixels exist our method will create blurry artifacts in the presentation of those events. Parts of the stream used in Fig. 18 suffer from blurry artifacts.

The final reconstruction artifacts are attributed to the lack

of events when the camera movement is parallel to the scene structure, therefore events will not fire. This artifact is generally available in all reconstruction methods based on pure events where we mention it for the sake of completeness. This artifact is shown in Fig. 19.

F. Extension to Video Reconstruction

We present our reconstructed images in a sequential manner to create a video. Our method does not focus on video reconstruction and mainly aims for single images, therefore the temporal consistency between frames are not always held. We utilize the method of [13] for creating the temporal relations among the intensity images and show it in the accompanied video.

G. Discussion on Overlapped Stacking and Higher Frame-rates (Section 3.1).

Based on the representation of the event stream stacked over time in Fig. 3 of the main paper, we are able to change the amount of overlap for stacking. This is expressed in Fig. 20 where the location of APS frames are shown and events can cover different amount of the time-line as stacks

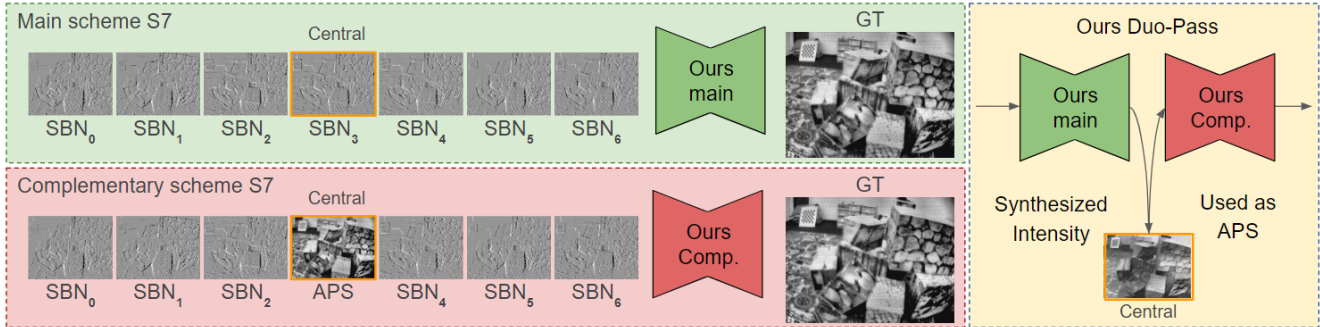


Figure 15. Main and complimentary (Comp.) scheme with $S7$ stacks in a sequence. The central stack is highlighted in the middle and all other stacks will be compared to this stack for optical flow creation. By putting the main network’s output from pure events as a LR input (central stack) for the Comp. network we can have the Duo-Pass network which can add more details to the original intensity image.

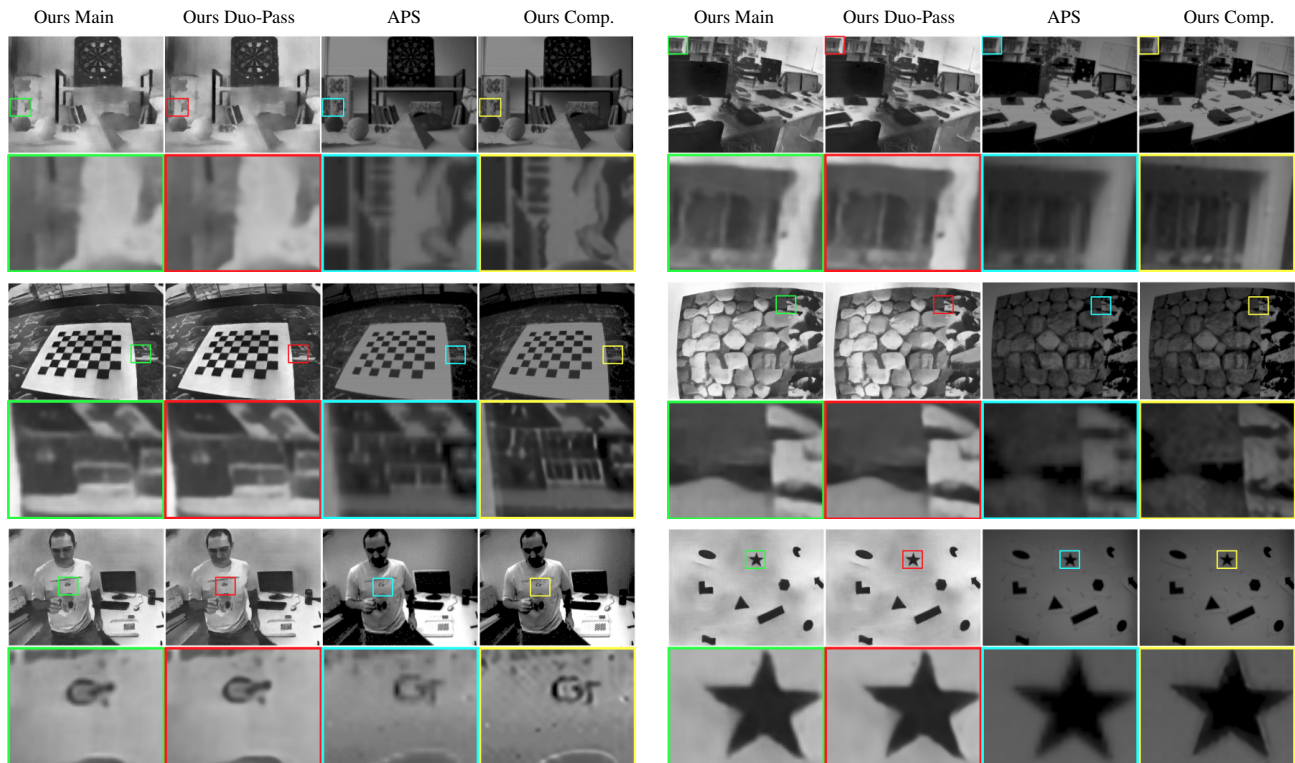


Figure 16. Further results of our main and extension methods: double passing (duo-pass) and complementary processing (comp.) using real-world events. Regions in the colored boxes are zoomed $20\times$ for comparison. APS frames that were very dark are histogram equalized for visualization only. Very high quality outputs can be achieved when complementing APS frames and events.

based on how fast the events are fired which is related to the camera or scene speed movement. This means that the size of the colored stacks or the overlaps are not necessarily equal to each other. Two stacks can have common events up to one single event. Unlike stacking based on time, stacking based on number of events (SBN) can consume different amount of time per stack which is related to the amount of events triggered from the scene. Furthermore it might even surpass the location of the previous or next APS frame location and is not bound to it. This overlap is useful when the scene movement is high and prevents short-time fired

events be less effective by having them in more than one stack over the total sequence of stacks.

In Fig. 20 the location of the APS is shown (as diamond shape) since it plays the role of the location where our reconstruction will be located on the time-line and is not used in any part of the reconstruction. At training the APS can be used as GT for training the network but at inference since it is not required to have the APS we can set an arbitrary point (shown as green circles) as the start point of our stack sequence. This point can have any wanted distance with the previous point making our algorithm to be

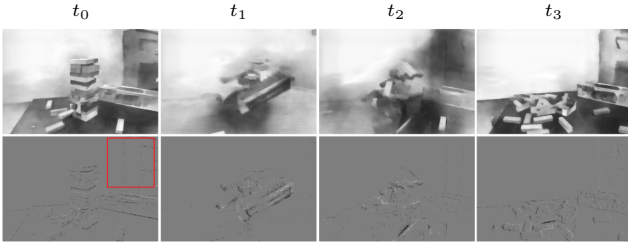


Figure 17. Forgetting background details in rapid object movement.



Figure 18. Foggy edges in the presence of noisy events.



Figure 19. Blur artifact due to lack of events.

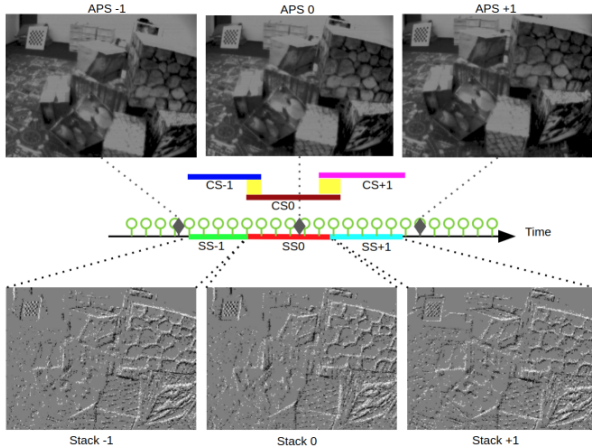


Figure 20. Stacking for training with regards to the GT (APS_0) frame (S_0 is the center stack). For testing any center point can be chosen however the naming of the next (+) or previous (-) stacks with regards to the center stack remains the same. The stacking can have overlapping events (Common Stacks CS) or be separate (Separate Stacks SS).

able to theoretically have unlimited frame rate. However the output reconstructed image will be almost identical to the previous image if the location are much nearby making the stacks have less difference. Therefore we recommend empirically to have at least a few hundred separate events over the stream. This extends our scheme from spatial only to space-time super-resolution, *i.e.*, creating higher frame-rates together with larger size outputs.

References

- [1] Patrick Bardow, Andrew J Davison, and Stefan Leutenegger. Simultaneous optical flow and intensity estimation from an event camera. In *Proceedings of the IEEE Conference on Computer Vision and Pattern Recognition*, pages 884–892, 2016. 1, 2, 6, 7, 10
- [2] Christian Brandli, Raphael Berner, Minhao Yang, Shih-Chii Liu, and Tobi Delbruck. A 240×180 130 db $3 \mu\text{s}$ latency global shutter spatiotemporal vision sensor. *IEEE Journal of Solid-State Circuits*, 49(10):2333–2341, 2014. 1, 2
- [3] Matthew Cook, Luca Gugelmann, Florian Jug, Christoph Krautz, and Angelika Steger. Interacting maps for fast visual interpretation. In *The 2011 International Joint Conference on Neural Networks*, pages 770–776. IEEE, 2011. 1, 2
- [4] Tao Dai, Jianrui Cai, Yongbing Zhang, Shu-Tao Xia, and Lei Zhang. Second-order attention network for single image super-resolution. In *Proceedings of the IEEE Conference on Computer Vision and Pattern Recognition*, pages 11065–11074, 2019. 2, 4, 6, 7
- [5] Daniel Gehrig, Antonio Loquercio, Konstantinos G. Derpanis, and Davide Scaramuzza. End-to-end learning of representations for asynchronous event-based data. In *Int. Conf. Comput. Vis. (ICCV)*, October 2019. 1, 3
- [6] Muhammad Haris, Gregory Shakhnarovich, and Norimichi Ukita. Deep back-projection networks for super-resolution. In *Proceedings of the IEEE conference on computer vision and pattern recognition*, pages 1664–1673, 2018. 4, 9
- [7] Muhammad Haris, Gregory Shakhnarovich, and Norimichi Ukita. Recurrent back-projection network for video super-resolution. In *Proceedings of the IEEE Conference on Computer Vision and Pattern Recognition*, pages 3897–3906, 2019. 2, 6, 7, 9
- [8] Kaiming He, Xiangyu Zhang, Shaoqing Ren, and Jian Sun. Deep residual learning for image recognition. In *Proceedings of the IEEE conference on computer vision and pattern recognition*, pages 770–778, 2016. 4
- [9] Eddy Ilg, Nikolaus Mayer, Tonmoy Saikia, Margret Keuper, Alexey Dosovitskiy, and Thomas Brox. FlowNet 2.0: Evolution of optical flow estimation with deep networks. In *Proceedings of the IEEE conference on computer vision and pattern recognition*, pages 2462–2470, 2017. 4
- [10] Michal Irani and Shmuel Peleg. Super resolution from image sequences. In *[1990] Proceedings. 10th International Conference on Pattern Recognition*, volume 2, pages 115–120. IEEE, 1990. 9
- [11] Hanme Kim, Ankur Handa, Ryad Benosman, Sio-Hoi Ieng, and Andrew J Davison. Simultaneous mosaicing and tracking with an event camera. *J. Solid State Circ.*, 43:566–576, 2008. 1, 2
- [12] Alex Krizhevsky, Ilya Sutskever, and Geoffrey E Hinton. Imagenet classification with deep convolutional neural networks. In *Advances in neural information processing systems*, pages 1097–1105, 2012. 5
- [13] Wei-Sheng Lai, Jia-Bin Huang, Oliver Wang, Eli Shechtman, Ersin Yumer, and Ming-Hsuan Yang. Learning blind video temporal consistency. In *European Conference on Computer Vision*, 2018. 11

- [14] Bee Lim, Sanghyun Son, Heewon Kim, Seungjun Nah, and Kyoung Mu Lee. Enhanced deep residual networks for single image super-resolution. In *Proceedings of the IEEE conference on computer vision and pattern recognition workshops*, pages 136–144, 2017. [2](#), [4](#)
- [15] Elias Mueggler, Henri Rebecq, Guillermo Gallego, Tobi Delbruck, and Davide Scaramuzza. The event-camera dataset and simulator: Event-based data for pose estimation, visual odometry, and slam. *The International Journal of Robotics Research*, 36(2):142–149, 2017. [1](#), [6](#), [8](#)
- [16] Henri Rebecq, Daniel Gehrig, and Davide Scaramuzza. Esim: an open event camera simulator. In *Conference on Robot Learning*, pages 969–982, 2018. [5](#)
- [17] Henri Rebecq, René Ranftl, Vladlen Koltun, and Davide Scaramuzza. High speed and high dynamic range video with an event camera. *arXiv preprint arXiv:1906.07165*, 2019. [1](#), [2](#), [4](#), [6](#)
- [18] Christian Reinbacher, Gottfried Graber, and Thomas Pock. Real-time intensity-image reconstruction for event cameras using manifold regularisation. In *British Machine Vision Conference*, 2016. [1](#), [2](#), [6](#)
- [19] Olaf Ronneberger, Philipp Fischer, and Thomas Brox. U-net: Convolutional networks for biomedical image segmentation. In *International Conference on Medical image computing and computer-assisted intervention*, pages 234–241. Springer, 2015. [2](#), [4](#)
- [20] Mehdi SM Sajjadi, Raviteja Vemulapalli, and Matthew Brown. Frame-recurrent video super-resolution. In *Proceedings of the IEEE Conference on Computer Vision and Pattern Recognition*, pages 6626–6634, 2018. [2](#), [4](#), [9](#)
- [21] Cedric Scheerlinck, Nick Barnes, and Robert Mahony. Continuous-time intensity estimation using event cameras. In *Asian Conference on Computer Vision*, pages 308–324. Springer, 2018. [1](#), [2](#), [6](#), [8](#)
- [22] Stepan Tulyakov, Francois Fleuret, Martin Kiefel, Peter Gehler, and Michael Hirsch. Learning an event sequence embedding for dense event-based deep stereo. In *Proceedings of the IEEE International Conference on Computer Vision*, pages 1527–1537, 2019. [1](#), [3](#)
- [23] Lin Wang, Mostafavi I. S. Mohammad, Yo-Sung Ho, and Kuk-Jin Yoon. Event-based high dynamic range image and very high frame rate video generation using conditional generative adversarial networks. In *Proceedings of the IEEE Conference on Computer Vision and Pattern Recognition*, pages 10081–10090, 2019. [1](#), [2](#), [4](#), [6](#)
- [24] Zhou Wang, Eero P Simoncelli, and Alan C Bovik. Multi-scale structural similarity for image quality assessment. In *The Thrity-Seventh Asilomar Conference on Signals, Systems & Computers, 2003*, volume 2, pages 1398–1402. Ieee, 2003. [6](#)
- [25] Richard Zhang, Phillip Isola, Alexei A Efros, Eli Shechtman, and Oliver Wang. The unreasonable effectiveness of deep features as a perceptual metric. In *Proceedings of the IEEE Conference on Computer Vision and Pattern Recognition*, pages 586–595, 2018. [5](#)
- [26] Alex Zihao Zhu, Dinesh Thakur, Tolga Özaslan, Bernd Pfrommer, Vijay Kumar, and Kostas Daniilidis. The multivehicle stereo event camera dataset: An event camera dataset for 3d perception. *IEEE Robotics and Automation Letters*, 3(3):2032–2039, 2018. [1](#), [6](#), [8](#)